SCIENTIFIC Publishing Limited

New Energy Exploitation and Application
http://ojs.ukscip.com/index.php/neea

Article

FEM Design and Analysis of PMBLDC Hub Motor for Electric Scooter

Mangaluru Satyendra Kumar Shet [1] ***and Shripad T. Revankar*** [2,*]

[1] Electrical Consultant, VAISHNAVI Electricals, Kodialgutthu(w), Mangaluru 575003, India
[2] School of Nuclear Engineering, Purdue University, West Lafayette, IN 47907, USA
[*] Correspondence: shripad@purdue.edu

Received: 10 March 2025; **Revised**: 15 May 2025; **Accepted**: 18 May 2025; **Published**: 25 May 2025

Abstract: This work presents design, performance evaluation and analysis of permanent magnet brushless direct current (PMBLDC) hub motor suitable for application to light electric vehicles (LEV) such as a scooter using finite element method (FEM). Designed for a 1.5 kW motor, the study addresses operational requirements of curb weight of 200 kg, speeds of 30–40 kmph, and the ability to ascend inclines up to 20^0. The customized motor design, power rating, and analysis is developed to match the requirements of the chosen appropriate vehicle parameters for the best possible torque-speed profile requiring least power. The design and analysis of the motor of the electric propulsion system applicable is capable for the Indian coastal topographical, urban and rural driving conditions. The analysis of the designed hub motor adheres to International Energy (IE) standards for IE3 performance efficiency. The study provides an insight in developing improved precise digital controller for high level accuracy and energy efficiency by incorporating advanced microelectronics and control techniques including artificial intelligence and machine learning. From this study and analysis, it has been observed that maximum torque density with small torque pulsation can be efficiently achieved for steady state, dynamic and ramp conditions with PI controller technique as the high-speed control accuracy and good dynamic responses are of vital importance for light electrical vehicle.

Keywords: PMBLD Hub Motor; Finite Element Method; Performance Evaluation; Electric Propulsion System; Torque-Speed Profile; Diverse Conditions; Vehicle Dynamics; Driving Conditions

1. Introduction

Zero emission transportation (ZET) with electrical vehicles is presently one of the measures to minimize the carbon dioxide footprints in atmosphere and arrest climate changes [1]. The technology of this type of system is a coordination, integration and optimization of different sub system components of the zero-emission vehicle namely the vehicle body structure, the electric propulsion system (EPS), energy storage system, and energy management system. The requirements of electric scooter are reliability, safety, precise accuracy in high-speed control, good dynamic response, noise pollution free, highly efficient with cost effectiveness and low maintenance. The challenges are: (a) Vehicle Characteristics, (b) Driving Cycle, (c) Vehicle Configuration, (d) Maximum Speed, (e) Maximum Torque, (f) Maximum Power, and (g) Battery as Energy Source. Successfully optimizing these multidisciplinary components requires addressing challenges such as weight, safety, reliability, and cost, while meeting the demands of diverse driving profiles and operational conditions.

Selection of electric motor for electric scooter application depends upon these above-mentioned points in addition to with or without gearbox and the cost [2]. Hence, suitable integration and coordination of all the sub system components of the LEV is of utmost importance to address the issues like weight, volume, driving profile, transport operating and temperature conditions, safety, reliability with cost economics [3,4]. The components of EPS are shown in **Figure 1.** This system primarily consists of motor, converter, controller unit and energy storage, among which motor is considered as "heart" of the EPS applicable to Electric Vehicle (EV).

Motors of the EPS operate at greater current density in comparison with the conventional motors of the same power rating that are used for standard industrial application. In general, electrical vehicle motors should have following special requirements:

1. Better performance in terms of efficiency for wide range of speed-torque.
2. Higher ratio of torque to power density, and higher initial torque for elevated acceleration and deceleration rates.
3. For starting and uphill climbing higher torque at low speeds and higher power at elevated cruising speeds.
4. Constant power and torque a for wide range of operating speed.
5. Easy-to-perform field-weakening at high speeds.
6. Small size and volume, lighter weight with high power and frequent starts/stops.
7. Good voltage regulation over a wide speed range and fast dynamic response.
8. High intermittent over load capability, typically twice the rated torque.
9. High reliability, robustness for harsh operating environments.
10. High fault tolerance operation and robust control.
11. Cost Economic and Rugged with simple maintenance
12. Low torque ripple, cogging torque and acoustic noise.
13. Minimum cooling requirements.
14. Mature technology, structural integrity and modular design.
15. Low level of electromagnetic interference (EMI) noise, minimum total harmonic distortion factor.
16. Water proof, shock proof, and dust proof.
17. Motor drive needs high controllability, steady-state accuracy, and good transient performance [5].

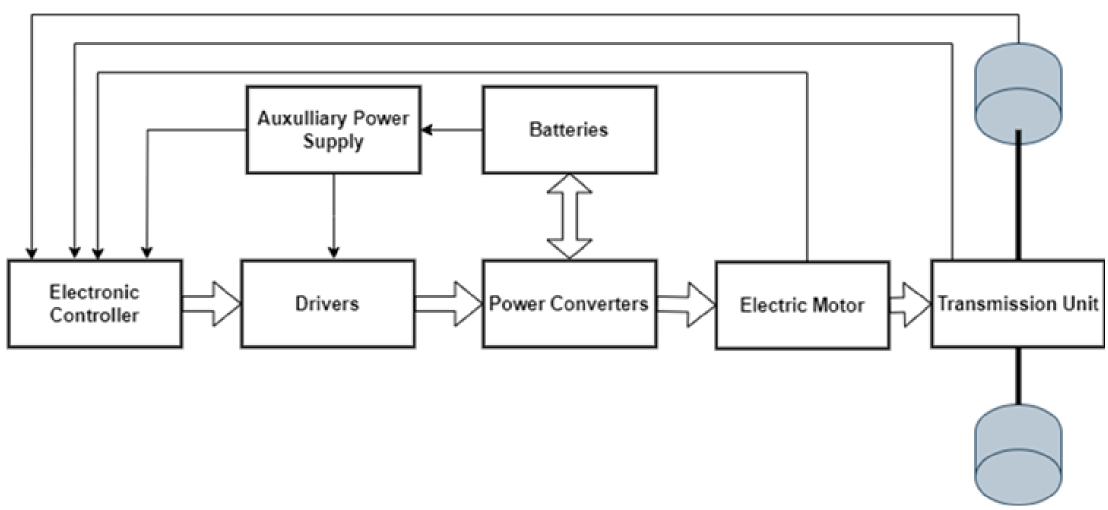

Figure 1. Key components of LEV Propulsion System.

The motor drive technology consists of power electronic converter of different topology namely inverter, dc-

dc converter, rectifier, with devices like MOSFET, IGBT, and SiC devices with control units of hard ware and software namely microprocessor (μp), microcontroller (μc),Digital Signal Processing (DSP), Fieldable Programme Group Array (FPGA), dspace, V/F control, Field Oriented Control (FOC), Direct Torque Control (DTC), Genetic Algorithm (GA), Artificial Neural Net (ANN) work, Fuzzy Logic (FL) Artificial Intelligence (AI) and Machine Learning (ML).

Recently PMBLDC motors have been developed with two most common types of rare earth Lanthanide series of magnets, Neodymium (Nd-Fe-B) and Samarium Cobalt (Sm-Co). As a result, these PMBLDC motors have become more capable of producing high power density and high efficiency when compared to the earlier DC and AC motors [6,7]. But they use electronic commutation with complex control algorithm.

LEVs have many different parts, but the major components ones are: batteries, brakes, controller, deck, handlebars, lights, motor, stem, suspension, and tires. Typically, Lithium-ion (Li-ion) rechargeable battery are used to drive the motor. The electric vehicle controller is the electronics package that operates between the batteries and the motor to control the LEV's speed and acceleration. Controllers adjust speed and acceleration by an electronic process called pulse width modulation. The controller receives the signal for the estimated power to be given for the intended load situation from zero to full power through the accelerator knob connected to a set of potentiometers or adjustable resistors [8,9].

In-wheel hub motor-drive system is preferable for electric scooter because wheel can be easily fixed over hub rotor or outer rotor-based configuration. The few benefits of PMBLDC motor are that they have quick dynamic response, higher efficiency, relatively high output power to their size, high-quality torque vs speed characteristics, fast dynamic response, and low noise operations [10,11]. The main challenges for PMBLDC motor-based LEV drive system are to enhance the motor efficiency and minimize the torque ripple. Requirement of higher motor driving current is a major constraint of the PMBLDC motor. The issues of PMBLDC-in-wheel motors are electromagnetic interference, torque ripple, noise, limited fault-tolerant capability, field weakening control, and relatively high cost of permanent magnets [12,13]. The main disadvantages of using this type of PMBLDC hub motor are (a) decrease in stability of the vehicle, because due to weight at the motor, (b) consistent in delivering steady torque is also not so easy and (c) mechanical stress [14–18].

The literature survey reveals that there are numerous numbers of research papers are already available that deals with different subsystems and its components of electric vehicle in terms of variety of technological developments, types and analysis [19–24]. These can be further classified as VBS, EPS [8,25–42], ESS [34,43–48] and EMS [49–56] respectively to mention the few. However, there is a lack of literature on state-of-art of holistic Electric Vehicle Technology (EVT) including detailed procedural steps towards design, development and analysis of the EPS and its suitability of integration in to electric vehicle application. There is also lack of clarity on standardization of specification of motor control units of the EV system.

Customized standards have been followed by several two-wheeler producing manufactures, such as battery operating voltage as 24 V and 48 V, power of battery ranging from 40 Ah to 100 Ah, and motor power up to 6 kW. Both sensor and sensor less motor controller units are used for PMBLDC hub motor drive.

Control system of PMBLDC motor is a multivariable nonlinear coupling system. The nonlinear control technique relies on state-of-the-art control theory and intelligent control algorithm, and is of complex type in comparison to the conventional PID control algorithm which is readily accessible. However, the rapid growth and advancement in modern power electronics, micro-electronics and control techniques has significant effect on PMBLDC motor drive because of the compact, integrated digital control technology. This digital control technology consists of high-speed processors and high-density PLC technology which provides assured reliable and feasible solution for electric scooter application. Complex control algorithms like FPGA, dspace, V/F, FOC, DTC, GA, ANN, Fuzzy Logic and AI etc. can be realized by means of this type digital control technology. Due to these advances, highly reliable, efficient dynamic and stable performance of the electric scooter drive can be achieved.

Various control techniques adopted are Field Oriented Control (FOC), Direct Torque Control (DTC), Intelligent Controller (IC), the duty cycle Model Predictive Control (MPC) and sensor less controller in order to overcome the torque ripple, reliability issues like fault-tolerant capability, EMI, acoustic noise, control problem in field weakening ability. Torque ripples in PMBLDC motors effects shaft failures, increased vibrations, and acoustic noises. For electric vehicle applications, these issues can be reduced by implementing advanced control techniques like FOC, DTC, and intelligent control [11]. The control techniques of FOC [57–58], DTC [59–63] and IC [64–66] are as shown in **Figure 2a–c** respectively used to reduce the torque ripple.

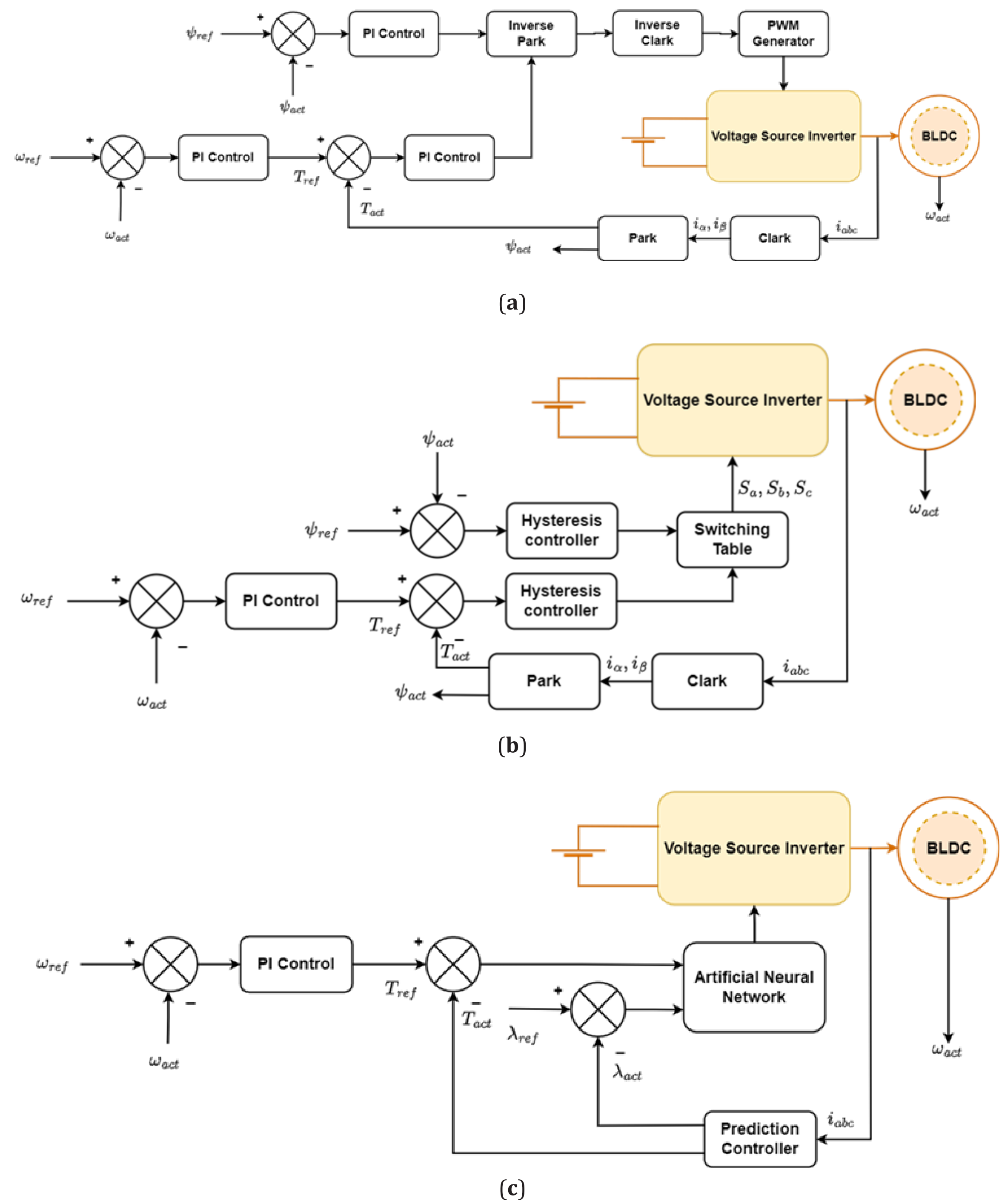

Figure 2. Control techniques for PMBLDC motor (**a**) Field-oriented control technique, (**b**) Direct torque control technique, (**c**) Intelligent control technique.

In MPC technique, offline model-based control is used for reducing the torque ripple. This method is sturdy and provides good dynamic response during the speed control [58,67,68]. For efficient fault-tolerant control, a model-based approach is mostly preferred. This model-based approach works on the principle of state estimation where the mathematical model of the system is predicted and the cost function (CF) estimation is performed.

Many researchers have discussed several topologies to reduce acoustic noise for PMBLDC motors both in design and motor-drive system control algorithm topology. Literature survey also reveals that there are also there are also other types of torque ripple reducing techniques namely Current Shaping Technique (CST) [65,69], Input Voltage Control (IVC) [70–71] technique, Sling Mode Control (SMC) [72] technique, Inverter Drive (ID) [73,74] topology and Modified PWM Control (MPC) technique [75–77].

In two-wheeler ZETS, the high-speed control accuracy and good dynamic responses are of vital requirement which can be suitably incorporated with PMBLDC hub motor-drive. This is because of the advancement in permanent magnet materials, power electronics, microelectronics and control [78]. The controller with control algorithms for the electric vehicle motor-drive is an intricate process with the cost limitation. The suitable smart precise controllers incorporating artificial intelligence (AI) and machine learning (ML) with sophisticated control algorithms techniques for this type motor-drive can also be developed.

This case study is focused on vehicle dynamics, calculations of power rating, choice of motor, design and performance evaluation of motor of the EPS applicable to electric scooter. The objective of study and analysis of this PMBLDC hub motor is to develop high power density, extensive speed range, high efficiency, good control, safety, ruggedness, with minimum power requirement to overcome the vehicle operational constraints, such that the developed motor is of less weight, compact, reliable, precise, cost effective and user friendly. Hence, the model developed can be suitably incorporated in real time application. The FEM design and analysis of 1.5 kW PMBLDC hub motor has been presented for the specified vehicle parameters, vehicle dynamics and driving cycle. From the simulation case study and analysis, it is observed that developed motor model meets all the requisite parameters of the vehicle dynamics and is in par.

The key contributions include: (a) A comprehensive design methodology using FEM to optimize structural and electromagnetic properties, (b) Analysis of the motor's torque, efficiency, and performance under various operational conditions, including inclines of up to 20° and (c) Evaluation of the motor's suitability for diverse urban and rural driving conditions. The findings contribute to developing efficient, scalable motor designs that align with the demands of sustainable mobility. Certainly, in today's context ZETS has become need of the society for both in urban and rural driving.

The aim is to validate the motor's suitability for the appropriate vehicle parameters, for the specific application mentioned, and not to benchmark against commercially available alternatives. Hence, comparisons with alternative hub motors or configurations involving mechanical components like external brackets and chain drives would introduce variables beyond the scope of this study. PMBLDC motors built with FEM offer high efficiency, compact size and lightweight, high torque and power density, low inertia, precise control performance, and reduced maintenance. These are essential requirements such safety, reliability, and cost of electric two-wheeler. But challenges are demagnetization, cogging torque, electronic control systems with sensor dependency and complex cooling requirements. But challenges are demagnetization, cogging torque, electronic control systems with sensor dependency and complex cooling requirements.

FEM provides precise modelling of complex geometries, including slot shapes and air gaps, and handles nonlinear material properties, anisotropy, and spatial field variations. Developed FEM model and analysis are focused on electromagnetic aspects such as magnetic flux density, cogging torque, winding behavior, and core saturation, also induced voltage, and efficiency for PMBLDC motor design parameters. Simulink, on the other hand, was used for system-level simulations, particularly for evaluating control strategies and converter interactions. FEM tool allows high-fidelity modelling of motor geometry and field distributions, which is critical for validating design assumptions that Simulink cannot capture in detail.

Organization of the paper is as follows. Section 2 illustrates PMBLDC motor topology and design of geometry dimension parameters for the motor power rating of 1.5 kW. FEM analysis of the motor drive system has been carried out. The software used is ANSYS's Maxwell design package. Motor dimensions are obtained and internal structure of the motor has been assessed. FEM outer rotor magnetic flux density, motor structure, analysis of the winding, mesh of the motor, flux density at the teeth, has been developed and analyzed. For the motor model, the voltage, current and induced emf, output torque, input DC current, output power and efficiency, cogging torque, no-load and full load torques have been generated and analyzed for the suitability of LEV application. Further by means of torque and speed profiles, the chosen motor capability for 0^0, 10^0, and 20^0, inclination has been assessed.

Section 3 provides the details of performance analysis of developed 1.5 kW PMBLDC hub motor model. This consists of analyzing the voltage, current, induced emf, output torque, input DC current, output power and efficiency, cogging torque, no-load and full load torques of the proposed 1.5 kW PMBLDC motor in order to find its feasibility for the LEV application. Further motor capability for 0^0, 10^0, and 20^0 inclinations also has been assessed by analyzing the torque and speed profiles.

In section 4, case study of the proposed motor design with results and analysis has been presented. For the reference speed signal of 1000 rpm, the analysis of back e.m.f, currents, and torques have been carried out, which indicates that the three phase back e.m.f's, currents and the torques are almost of trapezoidal shape of 120^0 difference. The load torque of 24 Nm is applied for 50 seconds. For 0^0 inclination the rotor no load speed profile, and for 10^0 and 20^0 inclinations with the load torque of 24 Nm, the rotor speed profile has been analyzed. This case study and analysis of the developed state-space model of the motor-drive has been assessed by MATLAB/Simulink.

In section 5, the details on the experimental setup for validation of the proposed propulsion system under real world condition is presented. In section 6, comprehensive data analysis, performance metrics and discussions are presented.

2. PMBLDC Hub Motor FEM Geometry Design

The objective of this FEM geometry design study is to develop high power density and high efficiency reliable PMBLDC hub motor with ruggedness for LEV application. Presently, several design possibilities are emerged in PMBLDC Motors [79–81] and its classification are as shown in **Figure 3a.** The design and construction are divided in to two parts namely: (a) stator and rotor and (b) inner rotor and outer rotor configurations. In case of outer rotor or hub motor configuration rotor permanent magnets are embedded at outer surface and stationary stator windings are housed in the peripheral as shown in **Figure 3b**. The construction and parts of such type of motor are shown in **Figure 3c**. The advantages of such type of design and construction are reduced weight, and volume, reduced air gap, increase in motor output torque, and power density and increase in stability of the rotor. Hence, during dynamic conditions the motor characteristics will be better. Thus, the outer rotor configuration of the PMBLDC motor is preferable for LEV applications. This type of in wheel motor is also called as hub motor.

Primary Propulsion System Design (PSD) for the vehicle parameters chosen are shown in **Table 1** and the corresponding power profile for the same is shown **Figure 4**, which suggest that 1.5 kW motor including the factor of safety margin at 25% with market standards is preferable. The power profile is obtained from the comparative study and analysis of two driving cycles, namely (a) New European Driving Cycle (NEDC) and Indian driving cycle (IDC) for the same duration of 1200 seconds. This is required to calculate the required motor power rating. In this case study it is of 1.5 kW. From this comparison it is observed that IDC data is suitable for the vehicle parameters of **Table 1** for Indian driving condition [80].

The PMBLDC motor of 3-phase, 1.5 kW, 4 pole rectangular waves, is considered for FEM geometry design. The distinct features of this design are: (a) reduction in magnetic yoke, (b) coil span equal to one slot pitch, and (c) number of slots per pole is fraction. As a result, there will be reduction in motor weight, size, reduction in copper mass, and reduction of cogging torque. Hub motor structure is considered in this design, where spokes of the wheel are directly accommodated into the outer rotor of this hub motor.

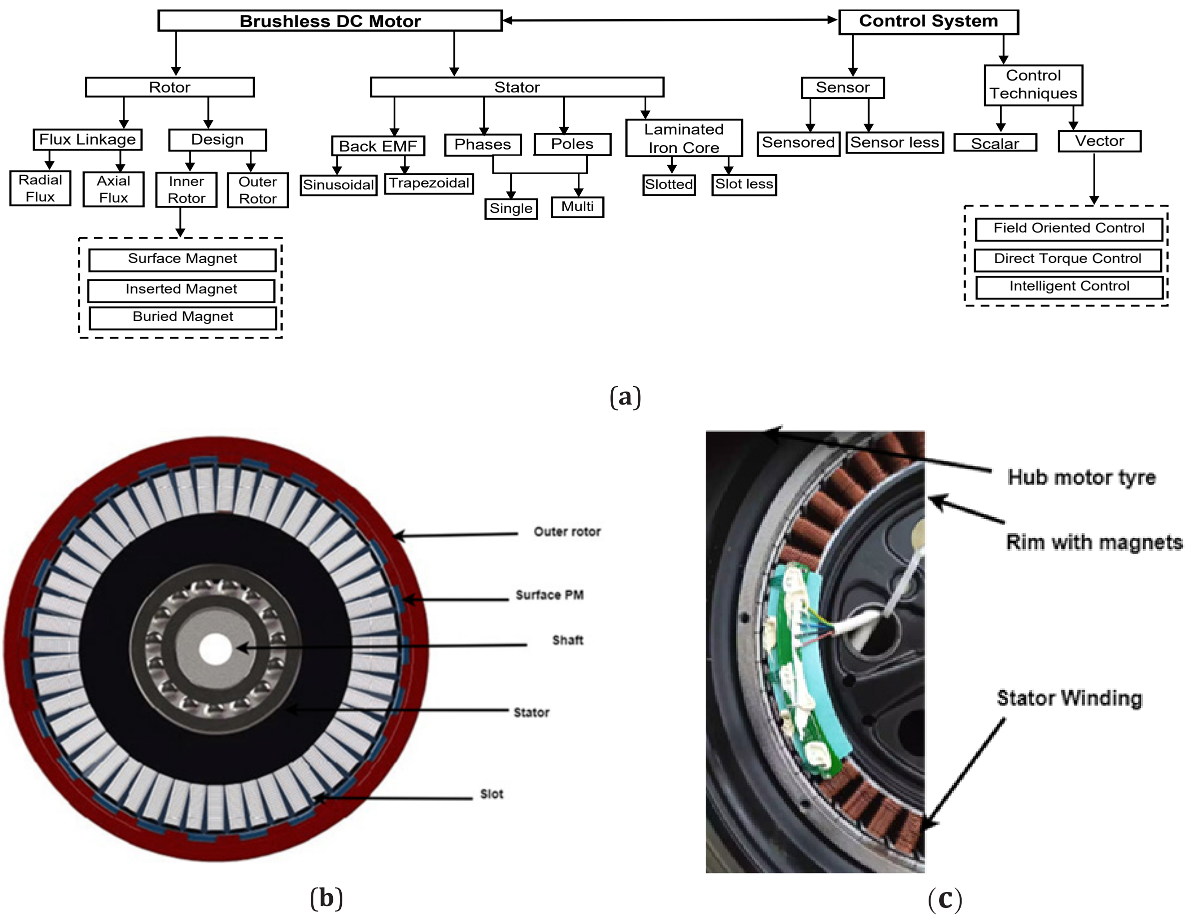

Figure 3. (**a**) BLDC motor design configuration options and control system, (**b**) Outer rotor configuration of PMBLDC motor, (**c**) Outer rotor type or Hub motor structure.

Table 1. Vehicle Parameters.

Sl.No.	Parameters (unit)	Value
1	Curb weight (kg) or mass of the LEV	200
2	Front area (m^2)	0.6
3	Velocity of the vehicle (km/h)	42
4	Density of the air at 20^0 C (kg/m^3)	1.204
5	Coefficient of rolling resistance	0.015
6	Drag coefficient	0.7
7	Tire diameter (mm)	416
8	Speed (km/h)	42
9	Capacity of gradient @ 10%	30
10	Capacity of gradient @ 20%	20
11	Maximum Acceleration (m/s^2)	0.65
12	Maximum Deceleration (m/s^2)	–0.63
13	Battery voltage (V)	48
14	Time for 1 cycle	108 sec's

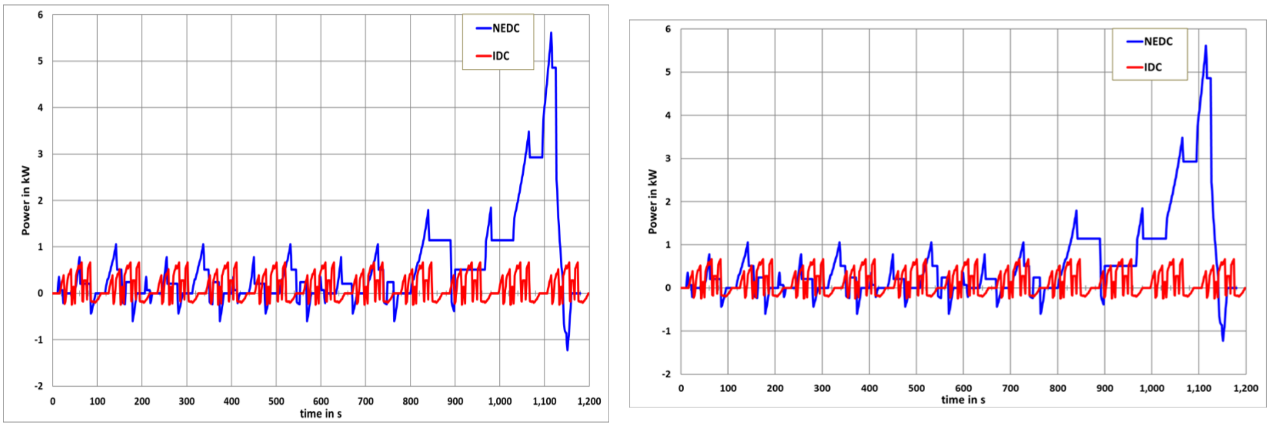

Figure 4. Vehicle motor power profiles for New European Driving Cycle (NEDC) and Indian driving cycle (IDC).

The design and optimization process of the motor involves analysis of electromagnetic field which is carried out using FEM. Due to its efficiency, 2D FEM is used to calculate torque production based on magnetic energy. This process is summarized as (a) Initializing the design and geometry of the configuration (b) Developing the meshes automatically for the area of association. (c) Evaluating the motor performance parameters and (d) by means of iteration modifying the geometry of the motor. The torque production depends on magnetic energy. Therefore, it is essential to formulate methods of computing it for which 2D FEM is suitable because of less memory storage and computation time in comparison to 3D calculation. The PMBLDC motor design parameters are shown in **Table 2.**

Table 2. PMBLDC motor design parameters.

Sl.No.	Parameters	Value
1.	Power	1.5 kW
2.	Voltage	48 V
3.	Rated current	46 A
4.	Rated torque	24 Nm
5.	Rated speed	1000 rpm
6.	Outer rotor/inner stator dia.	140 mm/111 mm
7.	Outer stator/inner rotor dia.	110 mm/50 mm
8.	Stack length	65 mm
9.	No. of slots	18 nos.
10.	Stacking factor	0.95
11.	Slot dimension	Optimized
12.	Rotor Magnet	NdFeB
13.	Stator steel	M19-29 G

The magnetic material neodymium ferrite boron (NdFeB) is a choice for rotor magnet which has high values of energy density, coercivity, remanence, and energy density. The stator steel is of M19-29 grade non-oriented silicon steel material which is laminated in the stator side, which has high energy density. For the motor dimensions like tooth width, bottom width, slot depth, back iron length, several iterations are made to optimize and select geometry parameters. In this hub motor design at rated speed either the rated current or the duty cycle will be minimum. For 360^0 rotation of the rotor maximum distribution of flux is 2.264 Tesla as shown in **Figure 5.** FEM

Motor structure details with parameters and winding analysis are shown in **Figures 6** and **7** respectively. Mesh generated for the FEM analysis of motor is shown in **Figure 8**.

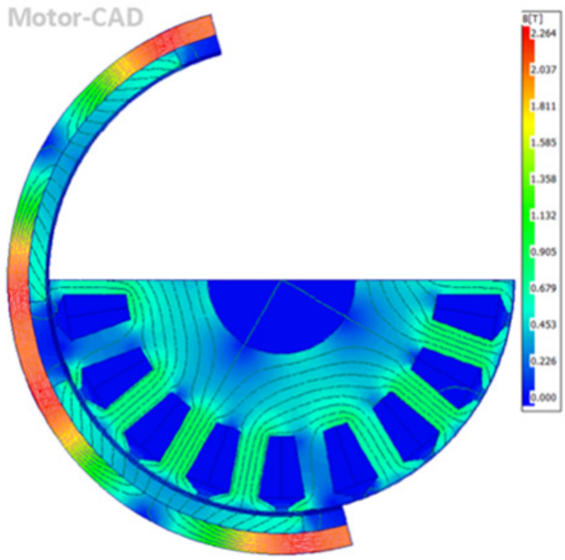

Figure 5. Finite Element outer rotor magnetic flux density.

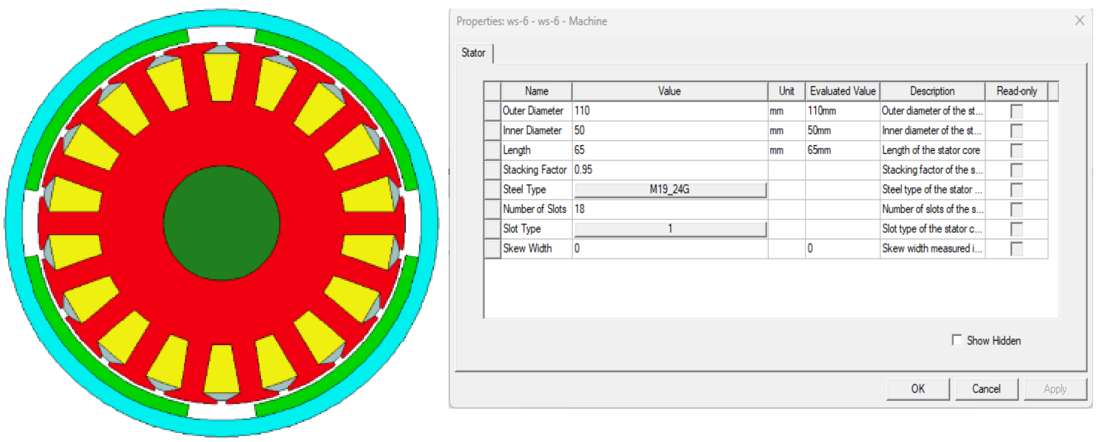

Name	Value	Unit	Evaluated Value	Description	Read-only
Outer Diameter	110	mm	110mm	Outer diameter of the st...	
Inner Diameter	50	mm	50mm	Inner diameter of the st...	
Length	65	mm	65mm	Length of the stator core	
Stacking Factor	0.95			Stacking factor of the s...	
Steel Type	M19_24G			Steel type of the stator ...	
Number of Slots	18			Number of slots of the s...	
Slot Type	1			Slot type of the stator c...	
Skew Width	0		0	Skew width measured i...	

Figure 6. Finite Element Motor Structure.

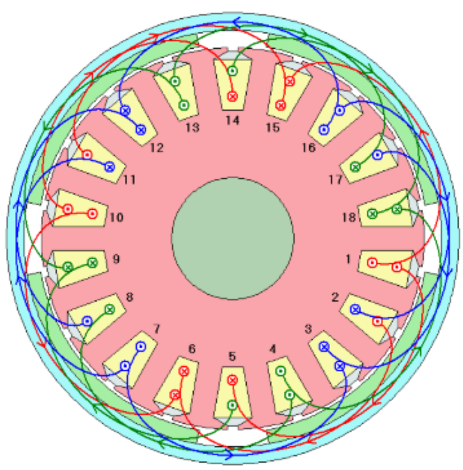

Figure 7. Finite Element Analysis of the Winding.

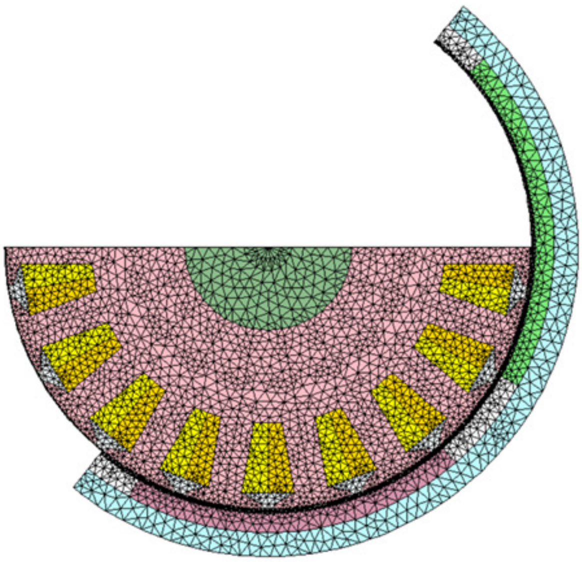

Figure 8. Finite Element Mesh of the Motor.

It is observed that at no-load condition, the flux density distribution symmetrical, whereas it is un-symmetrical at full load. This is because of the reaction of armature. The air gap flux distribution is required for the energy management process through the air gap. The normal and tangential component of flux density and force density all along the air gap periphery at full load condition is shown in **Figure 9**. Based on this result, motor geometry can be adjusted for the desired optimization.

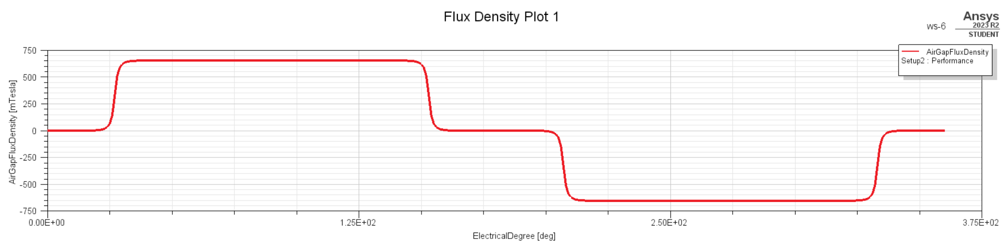

Figure 9. Air gap flux density distribution at the teeth.

3. Performance Analysis of 1.5 kW PMBLDC Hub Motor

The PMBLDC hub motor voltage, current and induced emf wave forms are as shown in **Figures 10a–c** respectively. The performance metrics including the motor output torque, input DC current and its performance, output power and efficiency performance graphs are as shown in the **Figure 11.** The cogging torque of the motor obtained is negligible as shown in **Figure 12**.

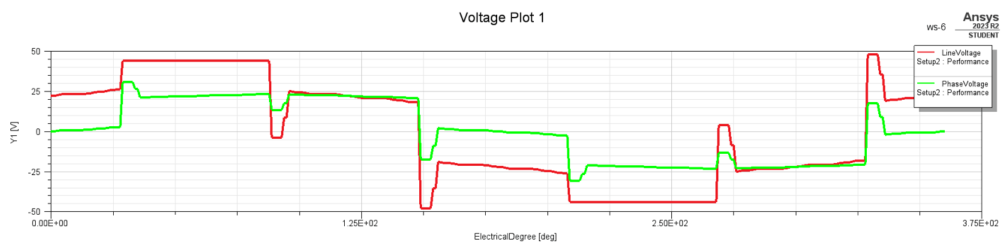

(a)

Figure 10. *Cont.*

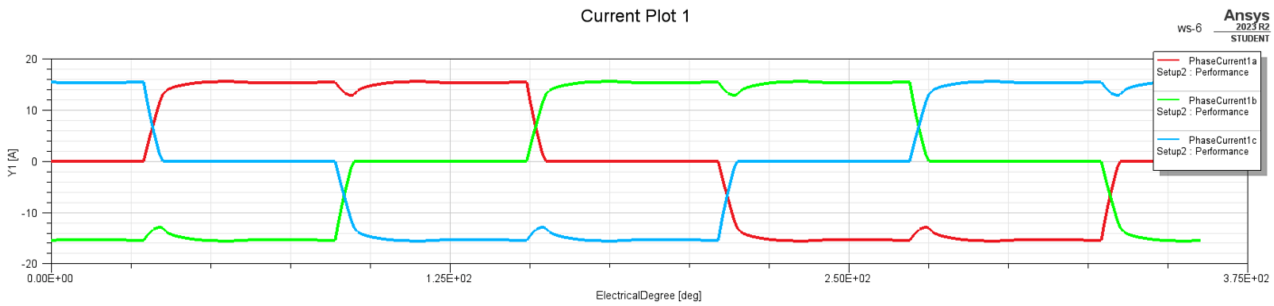

(**b**)

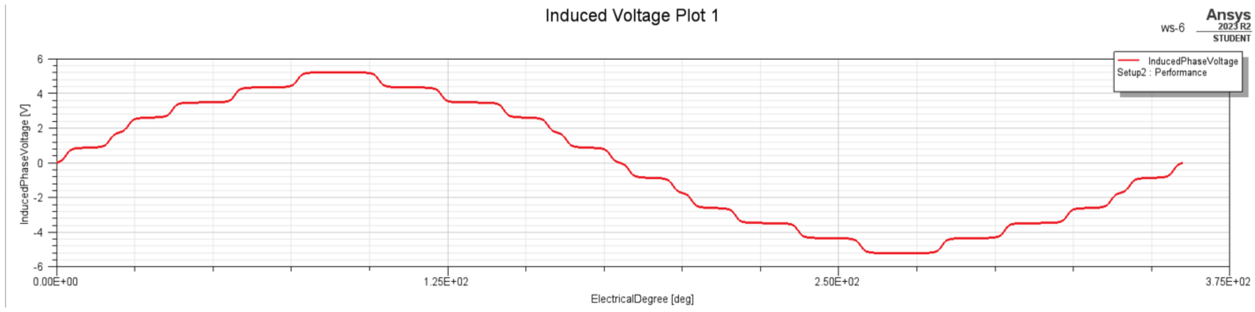

(**c**)

Figure 10. PMBLDC hub motor: (**a**) Voltage wave forms, (**b**) Current wave forms, (**c**) Induced voltage wave form.

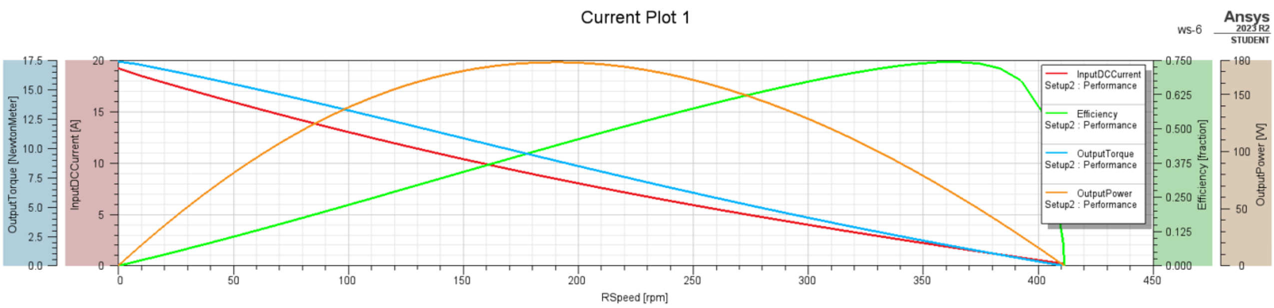

Figure 11. Output torque, input DC current, output power and efficiency performance wave forms.

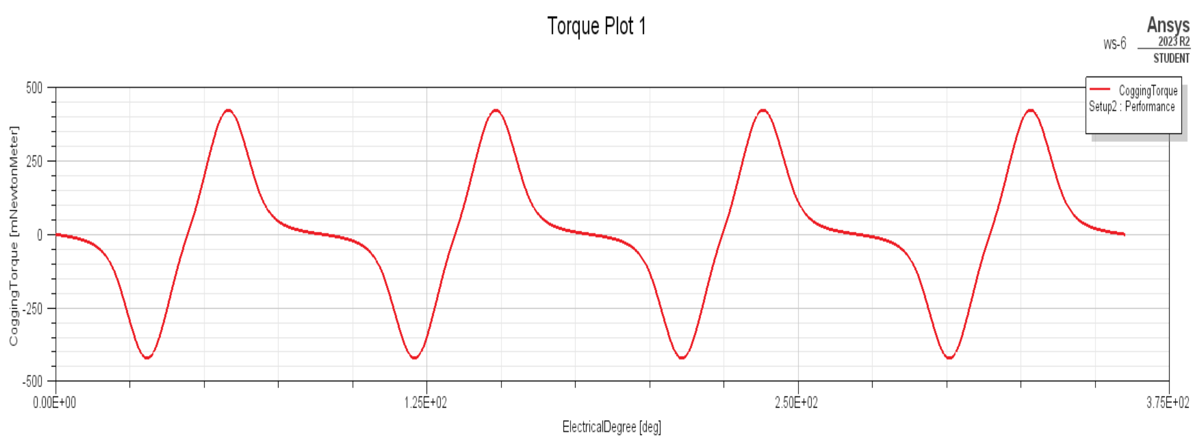

Figure 12. Cogging torque developed by the motor.

The no-load and full load torques developed by the PMBLDC motor is as shown in **Figure 13.** From this torque profile it is observed that for 0^0 inclination the torque developed by the motor at 40 km/h is 24 N-m, consistent with the vehicle parameters in **Table 1** and design parameters of **Table 2.** This confirms that chosen vehicle parameters of **Table 1** above, followed by motor parameters of **Table 2** above, both are in par for the LEV application. Hence, FEM geometry design and analysis demonstrates that the 1.5 kW PMBLDC hub motor is suitable for the chosen vehicle parameters of **Table 1**, which is also in par with vehicle dynamics and driving cycle chosen as above. The Torque vs. Time profile of the motor for 0^0, 10^0, and 20^0 inclination is as shown in **Figure 14**. Corresponding Speed vs. Time characteristics for 0^0, 10^0, and 20^0 inclination is as shown in **Figure 15.** For 10^0 inclination, the torque generated by the motor is reduced to 9 Nm which is applied for next 25 seconds with speed signal of 300 rpm. Hence, chosen 1.5 kW PMBLDC motor is also stable for 10^0 inclination. But for 20^0 inclination, the torque developed by the motor is further reduced and reaches negative region of –5 Nm which is applied for further 25 seconds and the motor become unstable, unable to maintain speed as shown in **Figures 14** and **15**. During this period the speed signal reaches zero as shown in **Figure 15.** This confirms that the chosen motor power rating and EPS is not capable for 20^0 inclination drive and hence the chosen PMBLDC motor of 1.5 kW becomes unstable and as a result it is not suitable for the chosen vehicle parameters of **Table 1** above. For steep inclines ≥ 20°, an upgraded motor with higher power and torque capacity is required.

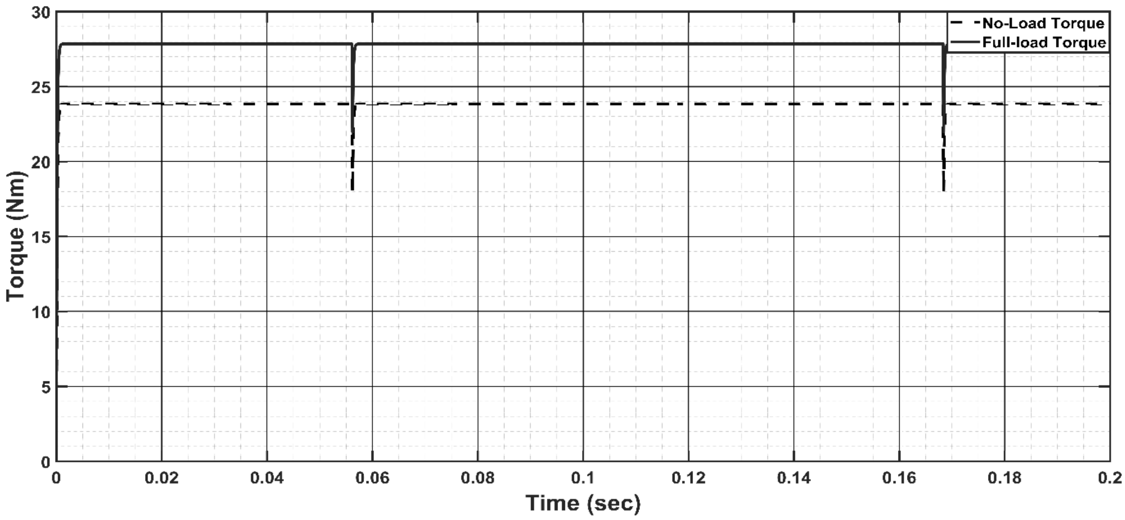

Figure 13. No-load and full load torques developed by the PMBLDC motor.

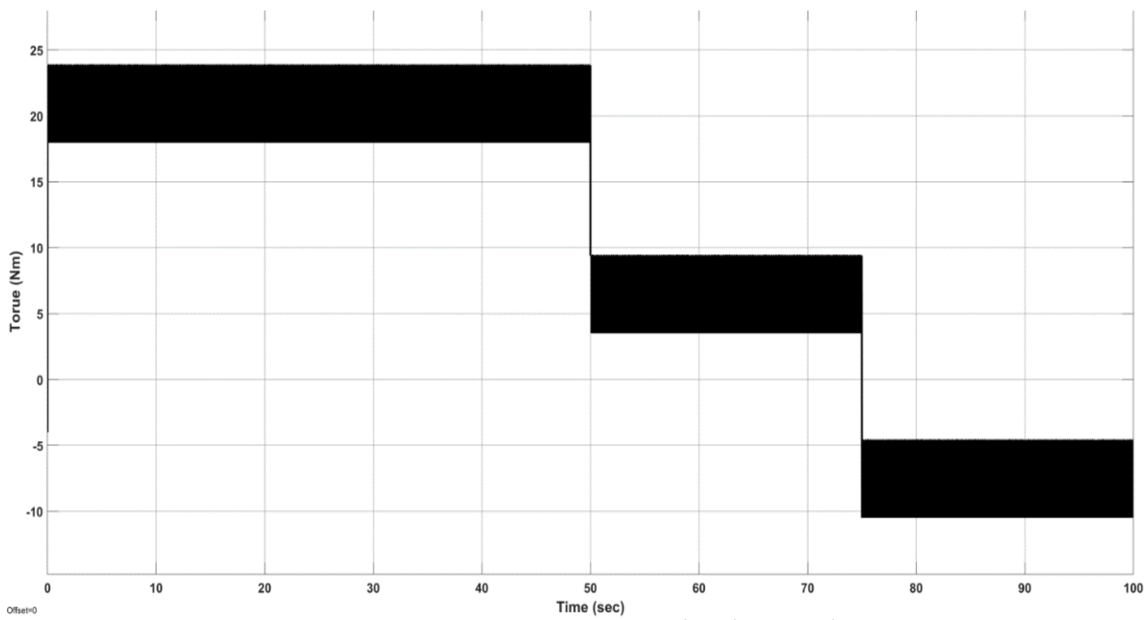

Figure 14. Torque vs. Time (sec) profile for 0^0, 10^0, and 20^0 inclinations.

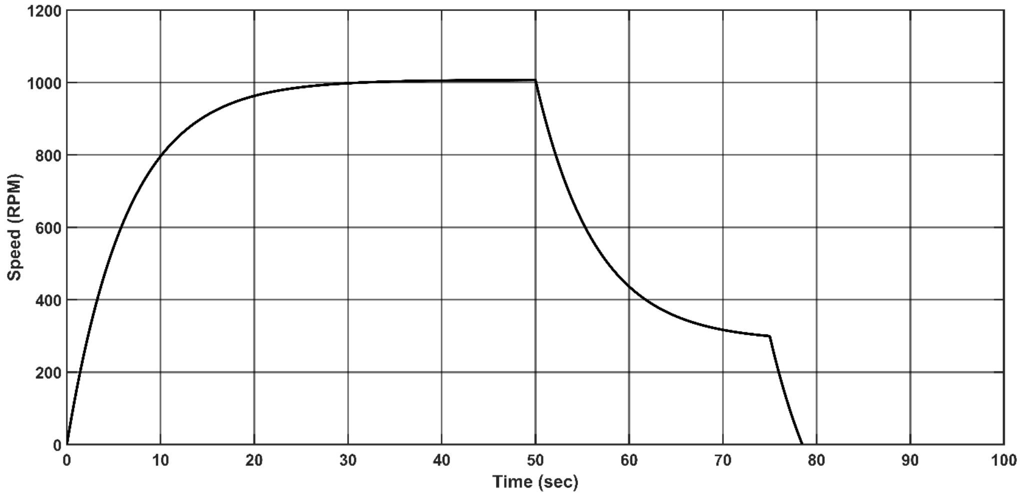

Figure 15. Corresponding speed profile of the PMBLDC motor for 0^0, 10^0, and 20^0 inclinations.

4. Electric Circuit Model of PMBLDC Hub Motor

For analysis torque performance, the PMBLDC motor with balanced three-phase, star connected, with symmetrical windings is chosen. The circuit model of the PMBLDC drive is as shown in **Figure 16**, in which the current commutation is achieved by means of six-step inverter with similar MOSFET switches. Voltage-fed inverters are virtually utilized since they are straightforward and allow power flow in either direction. Depending on the switching technique for various types of applications, its output waveform might be rectangular, six-step, or pulse-width modulation (PWM). The PWM waveform, is harmonically ideal and may have its basic magnitude and frequency smoothly changed to adjust speed. Several PWM switching schemes have been created for voltage-fed inverters over the past two decades, concentrating on harmonic suppression, greater dc voltage consumption, dc voltage tolerance, and appropriateness for real-time and digital control technique-based implementation.

Phase variables of three phase PMBLDC motor windings in matrix form for the balanced system is obtained by Kirchhoff' law to **Figure 17**, using the following assumptions.

1. Permanent magnet has high sensitivity.
2. Stator resistances of all the three windings are equal.
3. The induced currents in the rotor neglected.
4. The rotor reluctance does not change with angle.
5. Constant self and mutual inductance.
6. Motor is without damper windings.
7. Also, the high-power density with reduced weight and high efficiency with negligible cogging torque is achievable by means of multi-pole magnetic circuit with fractional slot geometry.

The voltage equations of the PMBLDC motor windings is given in equation (1).

$$\begin{bmatrix} v_a \\ v_b \\ v_c \end{bmatrix} = \begin{bmatrix} R & 0 & 0 \\ 0 & R & 0 \\ 0 & 0 & R \end{bmatrix} \begin{bmatrix} i_a \\ i_b \\ i_c \end{bmatrix} + \frac{d}{dt} \begin{bmatrix} L_a & L_{ba} & L_{Ca} \\ L_{ba} & L_b & L_{cb} \\ L_{ca} & L_{cb} & L_c \end{bmatrix} \begin{bmatrix} i_a \\ i_b \\ i_c \end{bmatrix} + \begin{bmatrix} e_a \\ e_b \\ e_c \end{bmatrix} \tag{1}$$

where V_a, V_b, and V_c are phase voltages of the stator windings, i_a, i_b, and i_c are stator phase currents, R_a, R_b, and R_c are the stator winding resistances, L_a, L_b, and L_c are per phase stator self inductances and L_{ab}, L_{bc}, and L_{ca} are the mutual inductances between the phases, e_a, e_b, and e_c, are the back e.m.f's which are the functions of rotor shaft angular velocity ω. Therefore, $e = K_e\omega$, where K_e is the back-emf constant in volt/(rad/sec).

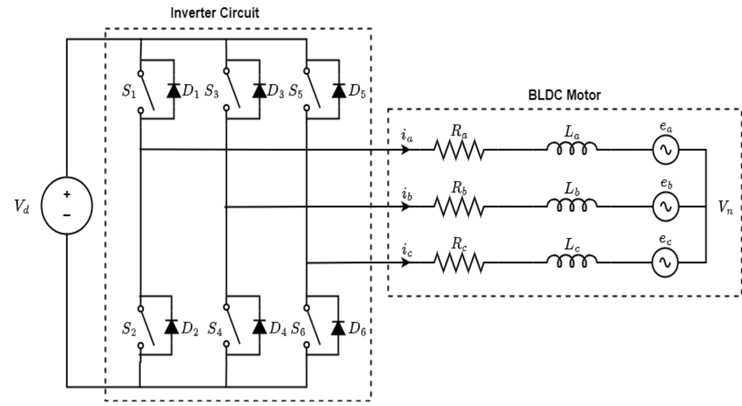

Figure 16. Electrical circuit representation of the chosen 3-phase PMBLDC motor.

In PMBLDC motor the induced electromotive forces are non-sinusoidal. Therefore, by using the phase variables mathematical model is developed.

The assumptions for the motor analysis by considering simplification and accuracy are as below:

1. The back e.m.f's e_a, e_b, and e_c, are of trapezoidal wave form,
2. Hysteresis and eddy current losses are neglected,
3. No Saturation,
4. Uniform air-gap, as a result, balanced stator current and self and mutual inductances are constant.

These assumptions lead to simplification of the inductance matrix in the model as: $R_a = R_b = R_c = R$, $L_a = L_b = L_c = L$ and $L_{ab} = L_{bc} = L_{ca} = M$.

The above equation (1) is simplified and further can be in state space form as shown in equation (2), in which, let $L\text{-}M = L_x$, and ω_a, ω_b, and ω_c, ω_c are angular speeds of rotor for electrical quantities of phases a, b and c, respectively.

$$\frac{d}{dt}\begin{bmatrix} i_a \\ i_b \\ i_c \end{bmatrix} = \begin{bmatrix} -\frac{R}{L_x} & 0 & 0 \\ 0 & -\frac{R}{L_x} & 0 \\ 0 & 0 & -\frac{R}{L_x} \end{bmatrix}\begin{bmatrix} i_a \\ i_b \\ i_c \end{bmatrix} + \begin{bmatrix} \frac{1}{L_x} & 0 & 0 \\ 0 & \frac{1}{L_x} & 0 \\ 0 & 0 & \frac{1}{L_x} \end{bmatrix}\begin{bmatrix} v_a \\ v_b \\ v_c \end{bmatrix} - \begin{bmatrix} -\frac{K_e}{L_x} & 0 & 0 \\ 0 & -\frac{K_e}{L_x} & 0 \\ 0 & 0 & -\frac{K_e}{L_x} \end{bmatrix}\begin{bmatrix} \omega_a \\ \omega_b \\ \omega_c \end{bmatrix} \tag{2}$$

Equation (2) can be writing in simplified for as equation (3):

$$\frac{d}{dt}\begin{bmatrix} i_a \\ i_b \\ i_c \end{bmatrix} = -\frac{R}{L_x}\begin{bmatrix} i_a \\ i_b \\ i_c \end{bmatrix} - \frac{1}{L_x}\begin{bmatrix} e_a \\ e_b \\ e_c \end{bmatrix} + \frac{1}{L_x}\begin{bmatrix} v_a \\ v_b \\ v_c \end{bmatrix} \tag{3}$$

The electromagnetic torque equation of PMBLDC motor is as given in equation (4) and in equation (s) as below:

$$T_e = \frac{(e_a i_a + e_b i_b + e_c i_c)}{\omega_r} \tag{4}$$

where T_e is Torque developed by the motor in N-m.

$$T_e = T_L + J\frac{d\omega_r}{dx} + B_m\omega_r \tag{5}$$

Rate of change of angular speed is given in equation (6)

$$\frac{d\omega_r}{dt} = \frac{(T_e - T_L - B\omega_r)}{J} \tag{6}$$

where T_L = load torque in N-m, B = frictional constant of motor in N-m/(rad/sec), and J = moment of inertia of motor and load in Kg-m^2/rad.

The electrical rotor speed and position are related by equation

$$\frac{d\theta_e}{dt} = \frac{P}{2}\omega_r \tag{7}$$

This motor modeling is required to analyze the performance of the EPS for a range of preferred speed and acceleration for desired angular displacements in vector control state-space and to calculate the maximum values of voltage and current during dynamic operating conditions of the EPS.

The above PMBLDC motor equations (3), (5), (6) and (7) in state space form is given by

$$\dot{x}(t) = Ax(t) + Bu(t) \tag{8}$$

where $\dot{x}(t)$ falsetime derivative of the state vector of the PMBLDC motor, A = matrix of the state of the PMBLDC motor; state variables $x(t) = [i_a, i_b, i_c, \omega_r, \theta_e]^T$, false B = Matrix of control PMBLDC motor and Input vector $u(t) = [v_a, v_b, v_c, T_L]^T$ false.

Generally, non-linear problem occurs when any one of the matrices in above equation (9) are time dependent and will have only exact solutions. In order to find the state equation, the above equation (9) is to be represented in discrete form with sampling interval, *T*, between k + 1 and k samples. The solution for the non-linear problem in discrete form is represented as below:

$$\frac{x_{k+1} - x_k}{T} = A_k x_k + B_k u_k \tag{9}$$

where A_k and B_k are constant at k and k = 0, 1, 2, 3, 4, 5, ...N.

The transition of the system from the state x_k to x_{k+1} is obtained from the above equation (9) and State Matrix A and Input B are given below:

$$\text{State Matrix A} = \begin{bmatrix} -\frac{R}{L_x} & 0 & 0 & -\frac{K_e}{L_x} & 0 \\ 0 & -\frac{R}{L_x} & 0 & -\frac{K_e}{L_x} & 0 \\ 0 & 0 & -\frac{R}{L_x} & -\frac{K_e}{L_x} & 0 \\ -\frac{K_e}{L_x} & -\frac{K_e}{L_x} & -\frac{K_e}{L_x} & -\frac{B}{J} & 0 \\ 0 & 0 & 0 & \frac{P}{2} & 0 \end{bmatrix}, \quad \text{Input Matrix } B = \begin{bmatrix} \frac{1}{L_x} & 0 & 0 & 0 \\ 0 & \frac{1}{L_x} & 0 & 0 \\ 0 & 0 & \frac{1}{L_x} & 0 \\ 0 & 0 & 0 & -\frac{1}{J} \\ 0 & 0 & 0 & 0 \end{bmatrix} \tag{10}$$

State space equation in discrete form is given by

$$x(k+1) = \begin{bmatrix} i_a(k+1) \\ i_b(k+1) \\ i_c(k+1) \\ \omega_r(k+1) \\ \theta_e(k+1) \end{bmatrix} = \begin{bmatrix} 1 - T\frac{R}{L_x} & 0 & 0 & -T\frac{K_e}{L_x} & 0 \\ 0 & 1 - T\frac{R}{L_x} & 0 & -T\frac{K_e}{L_x} & 0 \\ 0 & 0 & 1 - T\frac{R}{L_x} & -T\frac{K_e}{L_x} & 0 \\ -T\frac{K_e}{L_x} & -T\frac{K_e}{L_x} & -T\frac{K_e}{L_x} & 1 - T\frac{B}{J} & 0 \\ 0 & 0 & 0 & T\frac{P}{2} & 1 \end{bmatrix} \begin{bmatrix} i_a(k) \\ i_b(k) \\ i_c(k) \\ \omega_r(k) \\ \theta_e(k) \end{bmatrix} + \begin{bmatrix} T\frac{1}{L_x} & 0 & 0 & 0 \\ 0 & T\frac{1}{L_x} & 0 & 0 \\ 0 & 0 & T\frac{1}{L_x} & 0 \\ 0 & 0 & 0 & -T\frac{1}{J} \\ 0 & 0 & 0 & 0 \end{bmatrix} \begin{bmatrix} v_a(k) \\ v_b(k) \\ v_c(k) \\ T_L(k) \\ 0 \end{bmatrix} \tag{11}$$

where $i_a(k)$, $i_b(k)$, $i_c(k)$, $\omega_r(k)$ and $\theta_e(k)$ are the measured value of currents, angular velocity and displacement; whereas $\omega_r(k+1)$ and $\theta_e(k+1)$ are the planned values of angular velocity and the angular position of the motor shaft; T = sampling interval, time between $k + 1$ and k samples; R = the active resistance of the stator winding of the PMBLDC motor.

This state space drive model will provide information on the state of the system variables at few programmed positions along the path of the signal flow. As a result, greater flexibility and reliability with quick outcome is achieved by avoiding the powerful processor, and large Random-Access memory (RAM) and lengthy simulation time. These equations were solved using MATLAB/Simulink. The MATLAB/Simulink. Motor drive model with its system sub blocks are as shown in F**igure 17a–b** respectively.

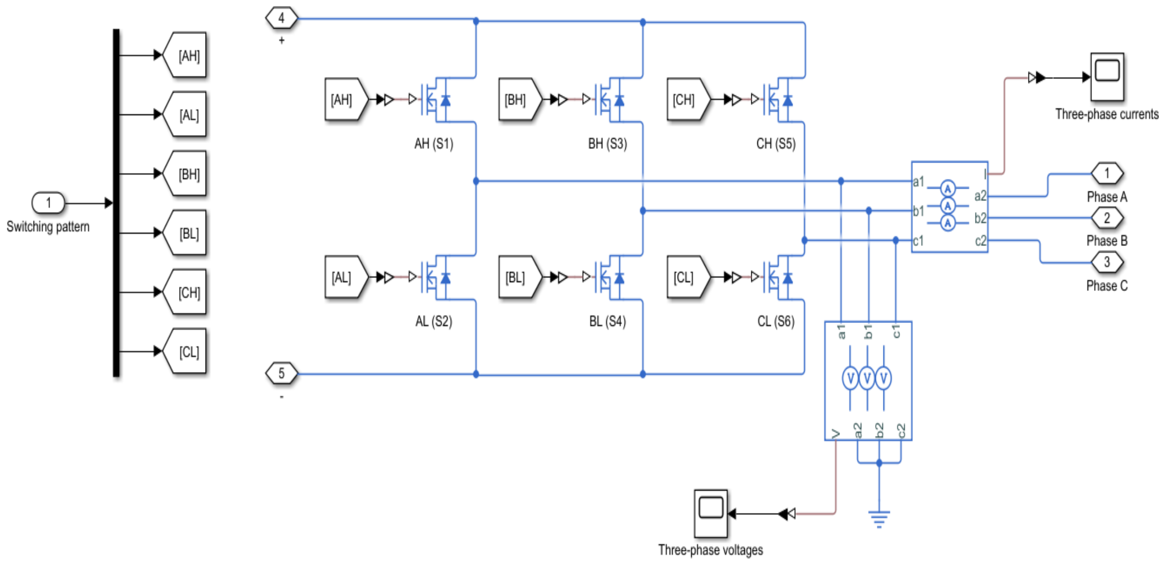

(**a**)

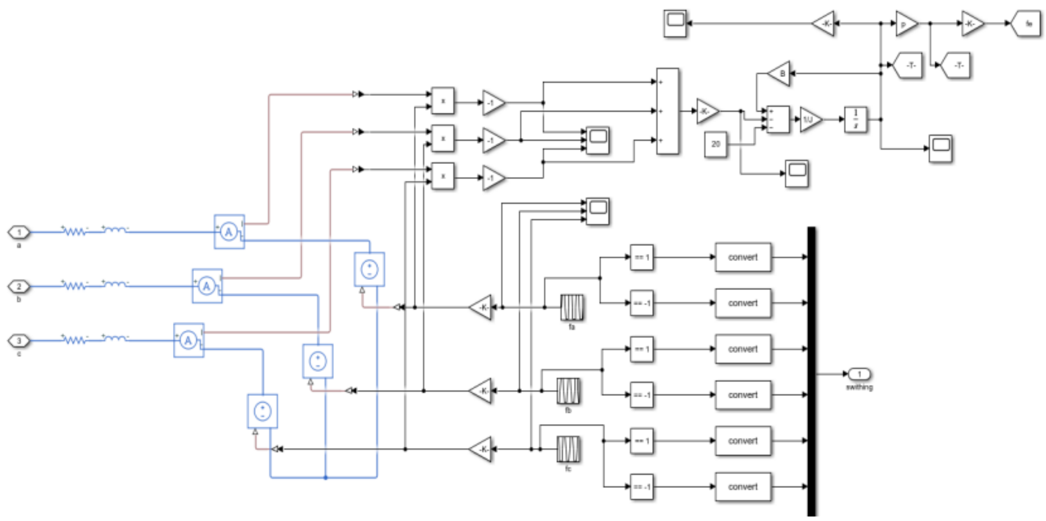

(**b**)

Figure 17. Simulink sub-blocks models of PMBLDC motor drive system to evaluate the performance of the designed motor, (**a**) electrical model of switching patters three phase input voltages and current fluxes, (**b**) three phase voltage and current measurements.

5. Case Study of the Design with Results and Analysis

This case study of the design and analysis of the motor-drive system is evaluated by MATLAB/Simulink with state-space model approach. It is a non-linear discrete model of the motor-drive system. In addition, the torque to be supplied based on performance investigation and the maximum values of voltage and currents during dynamic operating conditions of the EPS is also taken in to account by this technique. Technical parameters of the motor chosen for simulation case studies are shown in **Table 3,** which is as per the requirement of vehicle parameters of **Table 1** and PMBLDC hub motor design parameters of **Table 2** of previous section 2.

Table 3. Parameters chosen for case study.

Parameters	Particulars
Rated Voltage, V	48 Volts (DC)
Rated Power	1.5 k watts
Rated Torque	24 Nm
Rated Speed, N	1000 rpm
Stator Resistance, Ra	0.2 Ω
Stator Self inductance, La	1 mH
Mutual Inductances, M	0.2 mH
Back E.M.F per phase, e	42 V
Per Phase Current, irms	46.68 A
Back EMF	Trapezoidal
Back EMF constant, Ke	1.684 V/rad/s
Torque developed by the motor, Te (@ no-load)	24 N-m
Maximum Torque	48.9 N-m
Maximum Current	160.1 A
Torque constant, k_t	1.684 Nm/A
Moment of Inertia, J	0.00512 Kg/m^2

For the reference speed signal of 1000 rpm, back e.m.f's, currents, torques are as shown in **Figure 18a–c** respectively which indicates that the three phase back e.m.f's, currents and the torques are almost of trapezoidal shape of 120^0 difference. The load torque of 24 Nm is applied for 50 seconds. For 0^0 inclination the rotor no load speed profile is as shown in **Figure 18d.**

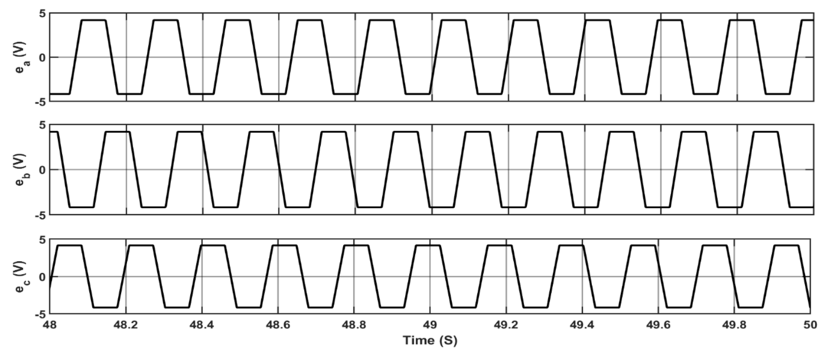

(**a**)

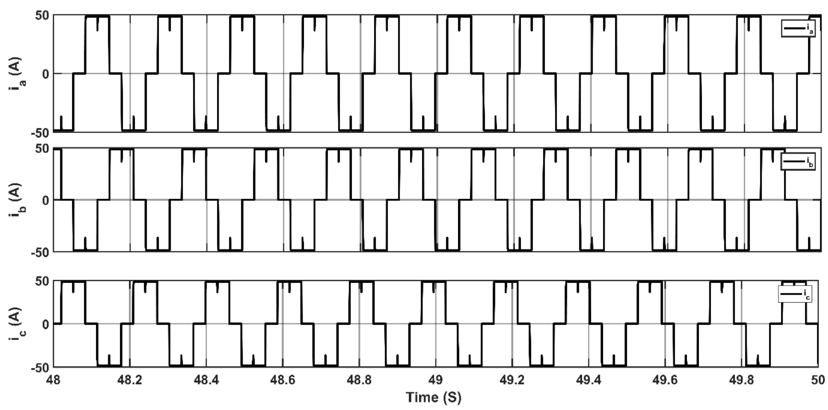

(**b**)

Figure 18. *Cont.*

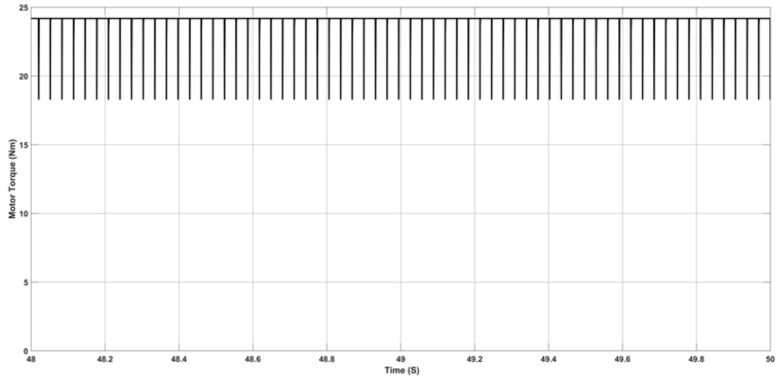

(**c**)

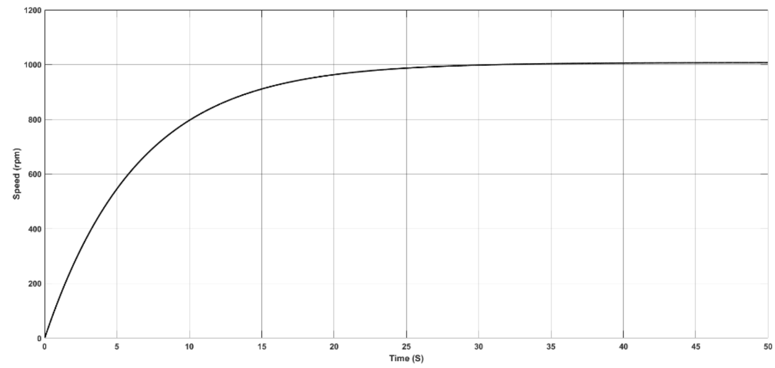

(**d**)

Figure 18. MATLAB/Simulink results on wave forms for reference design parameters shown in **Table 3**, (**a**) Back EMF Wave Form for 0^0 inclination, (**b**) Current Wave Form for 0^0 inclination, (**c**) Torque Wave Form for 0^0 inclination, (**d**) The rotor speed for 0^0 inclination with a load torque of 24 Nm.

At 0° Inclination the motor shows stable performance with a load torque of 24 Nm, as observed from the rortor speed profile in **Figure 18d.** For this load torque, the rotor speed reaches full value within 30 seconds and remails at 1000 rpm. When the Vehicle start climbing to 10^0 inclination after 50 seconds with the load torque of 24 Nm speed drops to 360 rpm from the reference speed of 1000 rpm as shown in **Figure 19**. The in drop in rotor speed is 64% when vehicle is climbing at 10^0 inclination at load torque of 24 Nm. When the Vehicle starts climbing to 20^0 inclination after 50 seconds with the load torque of 24 Nm, the speed drops to 0 rpm within next 8 seconds which is as shown in **Figure 20**, indicating 100% drop I rotor speed. This indicates that the vehicle fails to climb 20^0 and higher inclination.

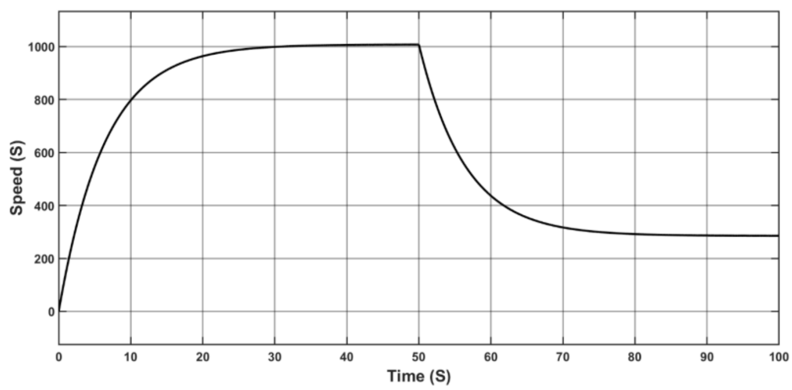

Figure 19. The motor rotor speed at 10^0 inclination with reference speed of 1000 rpm.

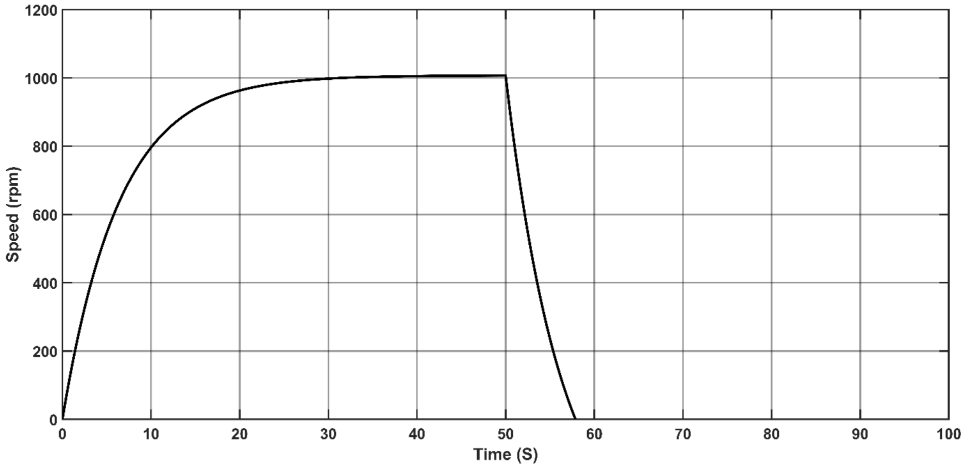

Figure 20. The motor rotor speed at 20^0 inclination with reference speed of 1000 rpm.

The study reveals that from 0^0 inclination up to 10^0 inclination of driving conditions the proposed designed system is stable though rotor speed drops and the vehicle speed is lower by 64%. To maintain vehicle speed as in 0^0 inclination, higher torque load is required. Since the rotor speed drops by 64% at least twice of load torque of 24 Nm may be required to have similar vehicle speed. But for inclination at and above 20^0 inclination of the driving conditions, it is unstable as the vehicle will certainly stall for given 24 Nm. For 20^0 and substantially higher load torque is required.

6. Experimental Validation

An experimental setup was designed to validate the proposed propulsion system under real-world conditions as shown in **Figure 21**. The testing environment was maintained at ambient temperatures of 25°C with controlled humidity. Key scenarios tested included hill climbing, stop-and-go traffic, and constant cruising speeds. It is observed that the input distortions eliminated, and smooth stability is achievable for driving conditions. The experimental results were as shown in **Figure 22a**,**b**, respectively. From **Figure 22b** it is observed that output current in the range of 20 A ripple content is restricted to 317 mA which indicates very minimal torque pulsation.

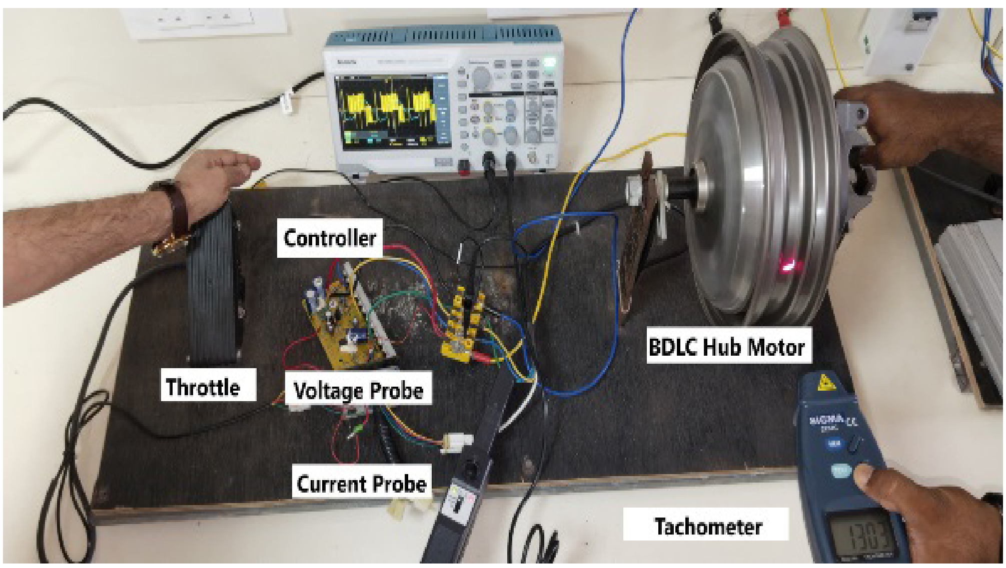

Figure 21. Experimental set up of PMBLDC hub motor drive.

(**a**)

(**b**)

Figure 22. (**a**) Speed at 250 rpm without load and with reduced accelerator, (**b**) Speed at 2000 rpm without load and with full accelerator.

The results from both simulation and experimental data analysis are summarized in **Table 4** that compares the key performance parameters such a Torque, output power and efficiency. The low percentage errors between simulation and experiential results indicate the high accuracy of the simulation model and validate its applicability for practical application.

Table 4. Comparison of experimental results with MATLAB/Simulink results.

Parameters	Simulation Result	Experimental Result	Percentage Error
Efficiency (%)	90.0	88.5	1.67%
Torque (Nm)	14.23	14.10	0.91%
Output Power (kW)	1.75	1.7	2.85%

The simulation and experimental results validate the proposed propulsion system design methodology employed here. Key performance metrics of the 1.5 kW PMBLDC motor under varied operational conditions are summarized as follows:

a. Efficiency: Achieves a peak efficiency of 90% at 1430 rpm, ensuring minimal energy losses.

b. Torque: Rated torque of 14.23 Nm is sufficient for overcoming gradients and drag forces.

c. Power: Maximum output power of 1.75 kW at 715 rpm, meeting acceleration and gradeability requirements.

d. Current: The input current profile demonstrates smooth operation with minimal distortions due to optimized control.

The study demonstrates the feasibility of the proposed methodology in addressing critical LEV propulsion challenges. Key insights from this include:

1. Wide-Range Constant Power Region: Operating in this region minimizes power requirements during acceleration and cruising, enhancing energy efficiency.
2. Gearless Design: The in-wheel motor configuration reduces weight and improves overall system efficiency, making it suitable for compact LEVs.
3. Real-World Validation: Simulation results align with experimental findings, ensuring reliability under practical conditions.

7. Conclusions

From the case study of FEM geometry design and analysis of PMBLDC hub motor, it is acknowledged that high power density with reduced weight and high efficiency, and negligible cogging torque is achievable by means of multi-pole magnetic circuit with fractional slot geometry. Various magnetic and electrical design aspects of PMBLDC hub motor have indicated that a 1.5 kW motor is best suited for EPS for use in Indian coastal topographical, urban and rural driving conditions. The EPS design is evaluated using a MATLAB/Simulink-based state-space model approach, which provides a non-linear discrete representation of the system. This method allows for detailed analysis of the torque requirements, as well as the voltage and current limits under different operating conditions. Using this transient model simulation results are presented on the performance of motor drive system torque for diffrener 10^0 and 20^0 degree inclination. The results indicate that the designed system is stable for driving at 10^0 inclination whereas for 20^0 and higher inclination it is unable. The analysis is supported with experimental validation. From experimental it is observed that output current in the range of 20 A ripple content is restricted to 317 mA which indicates very minimal torque pulsation.

Author Contributions

Conceptualization, M.S.K.S.; methodology, software, investigation, writing—original draft preparation, M.S.K.S.; writing—review and editing, M.S.K.S. and S.T.R.; visualization, M.S.K.S.; supervision, M.S.K.S. and S.T.R.; All authors have read and agreed to the published version of the manuscript.

Funding

This work received no external funding.

Institutional Review Board Statement

Not applicable.

Informed Consent Statement

Not applicable.

Data Availability Statement

No new data were created in this work.

Conflicts of Interest

The authors declare no conflict of interest.

References

1. Climate Change 2023: Synthesis Report. Available online: https://www.ipcc.ch/report/ar6/syr/downloads/report/IPCC_AR6_SYR_SPM.pdf (accessed on 6 May 2025).
2. Bertoluzzo, M.; Buja, G. Development of Electric Propulsion Systems for Light Electric Vehicles. *IEEE Trans. Ind. Inform*. **2011**, *7*, 428–435.
3. Chan, C.C. The state of the art of electric and hybrid vehicles. *Proc. IEEE* **2022**, *90*, 247–275.
4. Kumar, L.; Jain, S. Electric propulsion system for electric vehicular technology: A review. *Renew. Sustain. Energy Rev.* **2014**, *29*, 924–940.
5. Kumar, M.S.; Revankar, S.T. Development scheme and key technology of an electric vehicle: An overview. *Renew. Sustain. Energy Rev*. **2017,** *70,* 1266–1285.
6. Wang, Z.; Ching, T.W.; Huang, S.; et al. Challenges Faced by Electric Vehicle Motors and Their Solutions. *IEEE Access* **2021***, 9*, 5228–5249.
7. Poudel B.; Amiri, E.; Rastgoufard, P.; et al. Toward Less Rare-Earth Permanent Magnet in Electric Machines: A Review. *IEEE Trans. Magn.* **2021***, 57*, pp. 1–19.
8. Zhu, Z.Q.; Howe, D. Electrical Machines and Drives for Electric, Hybrid, and Fuel Cell Vehicles. Proc. *IEEE* **2007***, 95,* 746–765.
9. Ravi N.; Ekram, S.; Mahajan, D. Design and Development of a In-Wheel Brushless D.C. Motor Drive for an Electric Scooter. In Proceedings of 2006 International Conference on Power Electronic, Drives and Energy Systems, New Delhi, India, 12–15 December 2006.
10. Yang, Y.; Castano, S.M.; Yang, R.; et al. Design and Comparison of Interior Permanent Magnet Motor Topologies for Traction Applications. *IEEE Trans. Transp. Electrif.* **2017**, *3,* 86–97.
11. Mohanraj, D.; Aruldavid, R.; Verma, R.; et al. A Review of BLDC Motor: State of Art, Advanced Control Techniques, and Applications. *IEEE Access* **2022**, *10*, 54833–54869.
12. Krishnakumar, V.; Madhanakkumar, N.; Pugazhendiran, P.; et al. Torque ripple minimization of PMBLDC motor using simple boost inverter. *Int. J. Power Electron. Drive Syst.* **2019**, *10*, 1714–1723.
13. Shenoy K.L.; Kumar, M.S. Design topology and electromagnetic field analysis of Permanent Magnet Brushless DC motor for electric scooter application. *Int. Conf. Electr. Electron. Optim. Tech.* **2016**, 1541–1545.
14. Chau, K.T.; Zhang, D.; Jiang, J.Z.; et al. Design of a Magnetic-Geared Outer-Rotor Permanent-Magnet Brushless Motor for Electric Vehicles. *IEEE Trans. Magn.* **2007**, *43*, 2504–2506.
15. Krishnan, R. *Permanent Magnet Synchronous and Brushless DC Motor Drives,* 1st ed.; CRC Press: Boca Raton, FL, USA, 2017; pp. 457–563.
16. Pellegrino, G.; Vagati, A.; Guglielmi, P.; et al. Performance Comparison Between Surface-Mounted and Interior PM Motor Drives for Electric Vehicle Application. *IEEE Trans. Ind. Electron.* **2012**, *59*, 803–811.
17. Lee, T.-Y.; Seo, M.-K.; Kim, Y.-J.; et al. Motor Design and Characteristics Comparison of Outer-Rotor type BLDC Motor and BLAC Motor based on Numerical Analysis. *IEEE Trans. Appl. Supercond.* **2016,** *26*, p. 1–6.
18. Du, G.; Li, N.; Zhou, Q.; et al. Multi-Physics Comparison of Surface-Mounted and Interior Permanent Magnet Synchronous Motor for High-Speed Applications. *Machines* **2022**, *10*, 1–20.
19. Williamson S.S.; Emadi, A. Comparative assessment of hybrid electric and fuel cell vehicles based on comprehensive well-to-wheels efficiency analysis. *IEEE Trans. Veh. Technol.* **2005**, *54*, 856–862.
20. Gao, Y.; Ehsani, M.; Miller, J.M. Hybrid Electric Vehicle: Overview and State of the Art. In Proceedings of the IEEE International Symposium on Industrial Electronics, Dubrovnik, Croatia, 20–23 June 2005.
21. Amjad, S.; Neelakrishnan, S.; Rudramoorthy, R. Review of design considerations and technological challenges for successful development and deployment of plug-in hybrid electric vehicles. *Renew. Sustain. Energy Rev.* **2010***, 14*, 1104–1110.
22. Richardson, D.B. Electric vehicles and the electric grid: A review of modeling approaches, Impacts, and renewable energy integration. *Renew. Sustain. Energy Rev.* **2013***, 19*, 247–254.
23. Capuder, T.; Miloš Sprčić, D.; Zoričić, D.; et al. Review of challenges and assessment of electric vehicles integration policy goals: Integrated risk analysis approach. *Int. J. Electr. Power Energy Syst.* **2020***, 119*, 105894.
24. Ramesan, S.; Kumar, P.; Garg, S.K. Analyzing the enablers to overcome the challenges in the adoption of electric vehicles in Delhi NCR. *Case Stud. Transp. Policy* **2022***, 10*, 1640–1650.
25. West, J.G.W. DC, induction, reluctance and PM motors for electric vehicles. *Power Eng. J.* **1994***, 8*, 77–88.
26. Chan, C.C.; Chau, K.T. An overview of power electronics in electric vehicles. *IEEE Trans. Ind. Electron.* **1997**, *44*, 3–13.
27. Jahns, T.M.; Blasko, V. Recent advances in power electronics technology for industrial and traction machine drives. *Proc. IEEE* **2001***, 89*, 963–975.

28. Zeraoulia, M.; Benbouzid, M.E.H.; Diallo, D. Electric Motor Drive Selection Issues for HEV Propulsion Systems: A Comparative Study. *IEEE Trans. Veh. Technol.* **2006***, 55*, 1756–1764.
29. Lu, S.; Corzine, K.A.; Ferdowsi, M. A New Battery/Ultracapacitor Energy Storage System Design and Its Motor Drive Integration for Hybrid Electric Vehicles. *IEEE Trans. Veh. Technol.* **2007***, 56*, 1516–1523.
30. Shen, Z.J.; Omura, I. Power Semiconductor Devices for Hybrid, Electric, and Fuel Cell Vehicles. *Proc. IEEE* **2007***, 95*, 778–789.
31. Emadi, A.; Lee, Y.J.; Rajashekara, K. Power Electronics and Motor Drives in Electric, Hybrid Electric, and Plug-In Hybrid Electric Vehicles. *IEEE Trans. Ind. Electron.* **2008***, 55*, 2237–2245.
32. Zhu, Z.Q.; Chan, C.C. Electrical machine topologies and technologies for electric, hybrid, and fuel cell vehicles. In Proceedings of 2008 IEEE Vehicle Power and Propulsion Conference, Harbin, China, 3–5 September 2008.
33. Lee, Y.-J.; Khaligh, A.; Emadi, A. Advanced Integrated Bidirectional AC/DC and DC/DC Converter for Plug-In Hybrid Electric Vehicles. *IEEE Trans. Veh. Technol.* **2009***, 58*, 3970–3980.
34. Khaligh, A.; Li, Z. Battery, Ultracapacitor, Fuel Cell, and Hybrid Energy Storage Systems for Electric, Hybrid Electric, Fuel Cell, and Plug-In Hybrid Electric Vehicles: State of the Art. *IEEE Trans. Veh. Technol.* **2010***, 59*, 2806–2814.
35. Zhang, H., Tolbert, L.M.; Ozpineci, B. Impact of SiC Devices on Hybrid Electric and Plug-In Hybrid Electric Vehicles. *IEEE Trans. Ind. Appl.* **2011***, 47*, 912–921.
36. Song, B.-M.; Choi, J.-Y. A low-speed high-torque permanent magnet motor for electric scooters. In Proceedings of 2011 IEEE Vehicle Power and Propulsion Conference, Chicago, IL, USA, 6–9 September 2011.
37. de Santiago, J.; Bernhoff, H.; Ekergård, B.; et al. Electrical Motor Drivelines in Commercial All-Electric Vehicles: A Review. *IEEE Trans. Veh. Technol.* **2012***, 61*, 475–484.
38. Luo, Y.; Tan, D. Study on the Dynamics of the In-Wheel Motor System. *IEEE Trans. Veh. Technol.* **2012***, 61*, 3510–3518.
39. Karki, A.; Phuyal, S.; Tuladhar, D.; et al. Status of Pure Electric Vehicle Power Train Technology and Future Prospects. *Appl. Syst. Innov.* **2020***, 3*.
40. Madichetty, S.; Mishra, S.; Basu, M. New trends in electric motors and selection for electric vehicle propulsion systems. *IET Electr. Syst. Transp.* **2021***, 11*, 186–199.
41. Yilmaz, M.; Krein, P.T. Review of Battery Charger Topologies, Charging Power Levels, and Infrastructure for Plug-In Electric and Hybrid Vehicles. *IEEE Trans. Power Electron.* **2013***, 28*, 2151–2169.
42. Mastoi, M.S.; Zhuang, S.; Munir, H.M.; et al. An in-depth analysis of electric vehicle charging station infras6-tructure, policy implications, and future trends. *Energy Reports* **2022***, 8*, 11504–11529.
43. Chan, C.C.; Wong, Y.S.; Bouscayrol, A.; et al. Powering Sustainable Mobility: Roadmaps of Electric, Hybrid, and Fuel Cell Vehicles. *Proc. IEEE* **2009***, 97*, 603–607.
44. Whittingham, M.S. History, Evolution, and Future Status of Energy Storage. *Proc. IEEE* **2012***, 100,* 1518–1534.
45. Tie, S.F.; Tan, C.W. A review of energy sources and energy management system in electric vehicles. R*enew. Sustain. Energy Rev.* **2013***, 20*, 82–102.
46. Reddy, D.S.; Jeyaprabha, S.B. Modernized energy management system: A review. *J. Phys. Conf. Ser.* **2020**, *1706*.
47. Rimpas, D.; Kaminaris, S.D.; Aldarraji, I.; et al. Energy management and storage systems on electric vehicles: A comprehensive review. *Mater. Today Proc.* **2022***, 61*, 813–819.
48. Taghizad-Tavana, K.; Alizadeh, A.; Ghanbari-Ghalehjoughi, M.; et al. A Comprehensive Review of Electric Vehicles in Energy Systems: Integration with Renewable Energy Sources, Charging Levels, Different Types, and Standards. *Energies* **2023***, 16*.
49. Salmasi, F.R. Control Strategies for Hybrid Electric Vehicles: Evolution, Classification, Comparison, and Future Trends. *IEEE Trans. Veh. Technol.* **2007***, 56*, 2393–2404.
50. Pisu, P.; Rizzoni, G. A Comparative Study Of Supervisory Control Strategies for Hybrid Electric Vehicles. *IEEE Trans. Control Syst. Technol.* **2007***, 15*, 506–518.
51. Gurkaynak, Y.; Khaligh, A.; Emadi, A. State of the art power management algorithms for hybrid electric vehicles. In Proceedings of 2009 IEEE Vehicle Power and Propulsion Conference, Dearborn, MI, USA, 7–10 September 2009.
52. Çağatay Bayindir, K.; Gözüküçük, M.A.; Teke, A. A comprehensive overview of hybrid electric vehicle: Powertrain configurations, powertrain control techniques and electronic control units. *Energy Convers. Manag.* **2011***, 52*, 1305–1313.
53. Rezk, H.; Arfaoui, J.; Gomaa, M.R. Optimal parameter estimation of solar pv panel based on hybrid particle swarm and grey wolf optimization algorithms. In*t. J. Interact. Multimed. Artif. Intell.* **2021***, 6*, 145–155.
54. Shimin, V.V.; Shah, V.A.; Lokhande, M.M. A review on role of power electronics in electric vehicles: state-of-the-art and future trends. *J. CPRI* **2016***, 12*, 227–240.
55. Maroti, P.K.; Padmanaban, S.; Bhaskar, M.S.; et al. The state-of-the-art of power electronics converters configurations in electric vehicle technologies. *Power Electron. Devices Components* **2022**, *1*, 100001.
56. Hashemnia, N.; Asaei, B. Comparative study of using different electric motors in the electric vehicles. In Proceedings of the 2008 International Conference on Electrical Machines, Vilamoura, Portugal, 6–9 September 2008.
57. Sumega, M.; Rafajdus, P.; Stulrajter, M. Current Harmonics Controller for Reduction of Acoustic Noise, Vibrations and Torque Ripple Caused by Cogging Torque in PM Motors under FOC Operation. *Energies* **2020***, 13*.
58. Xia, K.; Ye, Y.; Ni, J.; et al. Model Predictive Control Method of Torque Ripple Reduction for BLDC Motor. *IEEE Trans. Magn.* **2018***, 56*, 1–6.
59. Zhao, W.; Lipo, T.A.; Kwon, B.-I. Torque Pulsation Minimization in Spoke-type Interior Permanent Magnet Motors With Skewing and Sinusoidal Permanent Magnet Configurations. *IEEE Trans. Magn.* **2015***, 51*, 1–4.

60. Liu, Y.; Zhu, Z.Q.; Howe, D. Commutation Torque Ripple Minimization in Direct Torque Controlled PM Brushless DC Drives. In Proceedings of Conference Record of the 2006 IEEE Industry Applications Conference Forty-First IAS Annual Meeting, Tampa, FL, USA, 8–12 October 2006.
61. Trivedi, M.; Patel, J. A DSC - Based field oriented control of SPMSM to mitigate practical difficulties with low resolution sxIncremental encoder. In Proceedings of 2014 International Conference on Computation of Power, Energy, Information and Communication (ICCPEIC), Chennai, India, 16–17 April 2014.
62. Castro, A.; Pereira, W.; Almeida; T.; et al. Improved Finite Control-Set Model-Based Direct Power Control of BLDC Motor with Reduced Torque Ripple. *IEEE Trans. Ind. Appl.* **2018**, *54*, 4476–4484.
63. Masmoudi, M.; Badsi, B.; Masmoudi, A. DTC of B4-Inverter-Fed BLDC Motor Drives With Reduced Torque Ripple During Sector-to-Sector Commutations. Power Electron. *IEEE Trans.* **2014**, *29*, 4855–4865.
64. Hakami, S.; Alsofyani, I.M.; Lee, K.-B. Torque Ripple Reduction and Flux-droop Minimization of DTC with Improved Interleaving CSFTC of IM fed by Three-level NPC Inverter. *IEEE Access* **2019**, *7*, 184266–184275.
65. Wang, Z.; Xie, S.; Guo, Z. A Complex Fuzzy Controller for Reducing Torque Ripple of Brushless DC Motor. In Proceedings of Emerging Intelligent Computing Technology and Applications, Ulsan, South Korea, 16–19 September 2009.
66. Lad, C.K.; Chudamani, R. Simple overlap angle control strategy for commutation torque ripple minimisation in BLDC motor drive. I*ET Electr. Power Appl.* **2018**, *12*, 797–807.
67. Çelik, E.; Ozturk, N. A new fuzzy logic estimator for reduction of commutation current pulsation in brushless DC motor drives with three-phase excitation. *Neural Comput. Appl.* **2019**, *31*, 1125–1134.
68. Yaya, S.; Honghua, W. Research on Reduction of Commutation Torque Ripple in Brushless DC Motor Drives Based on Fuzzy Logic Control. *Int. Conf. Comput. Intell. Secur.* **2009**, *1*, 240–243.
69. Jiang, W.; Wang, P.; Ni, Y.; et al. Multimode Current Hysteresis Control for Brushless DC Motor in Motor and Generator State With Commutation Torque Ripple Reduction. *IEEE Trans. Ind. Electron.* **2018**, *65*, 2975–2985.
70. Ho, Z.; Uang, C.; Wang, P.-C. Extracting DC bus current information for optimal phase correction and current ripple in sensorless brushless DC motor drive. *J. Zhejiang Univ. Sci. C* **2014,** *15*, 312–320.
71. Krishnan, G.; Ajmal, K.T. A neoteric method based on PWM ON PWM scheme with buck converter for torque ripple minimization in BLDC drive. In Proceedings of 2014 Annual International Conference on Emerging Research Areas: Magnetics, Machines and Drives (AICERA/iCMMD), Kottayam, India, 24–26 July 2014.
72. Viswanathan, V.; Jeevananthan, S. Hybrid converter topology for reducing torque ripple of BLDC motor. *IET Power Electron.* **2017**, *10*, 1572–1587.
73. Xu, Z.; Rahman, M.F. Comparison of a Sliding Observer and a Kalman Filter for Direct-Torque-Controlled IPM Synchronous Motor Drives. *IEEE Trans. Ind. Electron.* **2012**, *59*, 4179–4188.
74. Mahmoudi, H.; Aleenejad, M.; Ahmadi, R. Torque Ripple Minimization for a Permanent Magnet Synchronous Motor Using a Modified Quasi-Z-Source Inverter. *IEEE Trans. Power Electron.* **2019**, *34*, 3819–3830.
75. Peng, F.Z.; Shen, M.; Qian, Z. Maximum boost control of the Z-source inverter. *IEEE Trans. Power Electron.* **2004**, *1*, 255–260.
76. Zhang, X.J.; Chen, B.S. Influences of PWM mode on the current generated by BEMF of switch-off phase in control system of BLDC motor. In Proceedings of the Fifth International Conference on Electrical Machines and Systems (IEEE Cat. No.01EX501), Shenyang, China, 18–20 August 2001.
77. Basu, K.; Prasad, J.S.S.; Narayanan, G. Minimization of Torque Ripple in PWM AC Drives. *IEEE Trans. Ind. Electron.* **2009**, *56*, 553–558.
78. Floris, A.; Porru, M.; Damiano, A.; et al. Design of a High-Speed Electric Propulsion System for Electric Vehicles. In Proceedings of 2020 AEIT International Conference of Electrical and Electronic Technologies for Automotive (AEIT AUTOMOTIVE), Turin, Italy, 18–20 November 2020.
79. Rajagopal, K.R.; Chippa, S. Computer Aided Design and FE Analysis of a PM BLDG Hub Motor, Proce. In Proceedings of 2006 International Conference on Power Electronic, Drives and Energy Systems, New Delhi, India, 12–15 December 2006.
80. Hsin-Chang, C.; Rohman, Y.F.; Ashlah, M.B.; et al. Electrification of Agricultural Machinery: One Design Case of a 4kW Air Compressor. *Energies* **2024**, *17*, 1–24.
81. Tosun, O.; Serteller, N.F.O. The Design of the Outer-Rotor Brushless DC Motor and an Investigation of Motor Axial-Length-to-Pole-Pitch Ratio. *Sustainability* **2022**, *14*, 12743.